Journal of Energy Storage 42 (2021) 102966

Contents lists available at ScienceDirect

Journal of Energy Storage

journal homepage: www.elsevier.com/locate/est

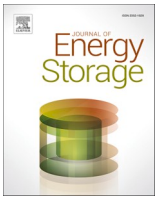

Electric vehicle charging and discharging scheduling strategy based on local search and competitive learning particle swarm optimization algorithm

Wan-Jun Yin, Zheng-Feng Ming *

School of Mechano-Electronic Engineering, Xidian University, Xi,an 710071, P.R. China

ARTICLE INFO

Keywords:
Electric vehicle
Power grid
Multi-objective optimization
SW-OBLCSO algorithm

ABSTRACT

It is great significance for environmental protection, energy conservation and emission reduction to replace fuel vehicles with EVs(electric vehicles).However, as a kind of random mobile load, large-scale integration into the power grid may lead to power quality problems such as line overload, line loss increase, voltage reduction and so on. In order to minimize the adverse effect of the disordered charging of EVs on the distribution grid, this paper takes the typical IEEE-33 node distribution system as the research object, a backward learning competitive particle swarm optimization (PSO) algorithm based on local search (SW-OBLCSO) is proposed. The SW-OBLCSO algorithm competitive learning and reverse learning mechanisms. In order to verify the performance of the algorithm, 4 common test functions are used, test functions compare the SW-OBLCSO algorithm with multiple optimization algorithms in different dimensions. The experimental results show that the proposed algorithm has outstanding performance in convergence speed and global search ability. This paper takes the minimum operation cost, the minimum environmental pollution, the minimum peak valley difference of load, the minimum node voltage offset rate, the minimum system grid loss and lowest charge cost as the optimization objectives; results shows that the proposed scheme can realize the transfer of charging load in time and space, so as to stabilize the load fluctuation of distribution grid, improve the operation quality of power grid, reduce the charging cost of users, and achieve the expected research objectives.

1. Introduction

With the application of fast charging technology, the rapid charging of EVs will become the future development mainstream direction [1]. Since the fast charging power far exceeds the power of conventional charging, the load change caused by the rapid charging of the EV may further aggravate the peak-to-valley difference of the grid load, causing overloading of the distribution grid, voltage drop, increase of distribution grid loss, and power distribution. For transformer overload problems, it is necessary to study the characteristics of fast charging power, saturation law and large-scale charging characteristics of large-scale electric vehicle clusters, so as to provide theoretical support for the optimal design of electric vehicle charging station grid [2]. Therefore, it is of great significance to study the rapid charging characteristics of EVs [3].

The disordered charging of large-scale EVs, if not controlled, the charging load of EVs will coincide with the peak load of the grid [4–8], forming a new peak of load, bringing a big impact to the grid; in the trough, the energy is largely idle [9], It is not conducive to the reliable operation of the power grid [10], but also creates expensive investment problems [11]. In addition, the battery of an electric vehicle is used as an energy storage device. During the peak period of the grid load, the grid load can be stabilized by discharging to the grid. Therefore, studying the orderly charge/discharge management of EVs has great significance for the development and application of EVs [12].

Because the orderly charging of EVs is a nonlinear and multi-constrained optimization problem, some classical optimization algorithms such as gradient, Hessian matrix, Lagrange discount [13,14], and multiplier method are not applicable [4]. PSO algorithm [2] has the advantages of strong applicability, easy convergence, high search efficiency [15–20], and does not require continuous differentiable optimization function, so it is very suitable for solving multi-modal and high-dimensional problems [21–23]. In the PSO algorithm, improving or introducing a more intelligent learning mechanism to improve the

* Corresponding author.
E-mail addresses: 514186187@qq.com (W.-J. Yin), zfming@xidian.edu.cn (Z.-F. Ming).

https://doi.org/10.1016/j.est.2021.102966
Received 26 November 2020; Received in revised form 18 July 2021; Accepted 19 July 2021
Available online 5 August 2021

performance of the algorithm has always been a research hotspot. Literature [12] combined the directional drift motion of free electrons in metal conductors, proposed the Random Drift Particle Swarm Optimization (RDPSO).Opposition-Based Learning (OBL) as an effective mechanism to broaden the search space [13,14], it has been effectively applied to the PSO algorithm. Literature [15] proposed a neighborhood center of gravity OBL particle swarm optimization algorithm, so as to make full use of the group search experience while maintaining the diversity of the population. The above two improved algorithms based on PSO do not pay attention to the high-dimensional scalability of the algorithm. Literature [16,17] introduced the OBL algorithm into the competitive PSO optimization algorithm, during the competition, some particles update their positions through reverse learning, this algorithm has a good performance on high-dimensional problems. In the Chicken Swarm Optimization (CSO) algorithm [24], chicken particles tend to converge prematurely, fall into local optimality and fail to achieve global optimality. Quantum-behaved Particle Swarm Optimization (QPSO) algorithm [25] also has a premature trend, when the group evolves, the diversity of the group inevitably decreases, so that the solution falls into the local optimum. In the Social Learning PSO (SL-PSO) [26] algorithm, the particles are updated based on historical information, including the best solution found by the entire group (global best) and the best solution found by each particle (personal best), but SL-PSO only performs well on low-dimensional problems, and its performance is poor for high-dimensional optimization algorithms.

Based on this, this paper takes the large-scale EVs into the grid as the background, fully considers power balance of the distribution network [27–29], optimal power flow and voltage constraints factors, starting from economic and environmental benefits, it takes the lowest operating cost of the distribution network, the lowest carbon emissions, the smallest load peak-to-valley difference, the smallest grid loss, and the user's total charging cost as the optimization objective function, on the basis of improving the competitive PSO algorithm, in order to achieve a better balance between the algorithm's global search ability and local search ability, the reverse learning mechanism and local search strategy are integrated, a backward learning competitive particle swarm optimization algorithm based on local search (SW-OBLCSO) is proposed. The improved competition mechanism combined with the reverse learning mechanism improves the convergence speed of the algorithm. In the later stage of the search, the individual-based Solis&Wets [18] local heuristic search operator is combined to help the algorithm jump out of the local optimal solution. So as to realize the orderly interaction between large-scale electric vehicles and the power grid.

Our contributions are summarized as follows.

Based on the PSO algorithm, a SW-OBLCSO algorithm based on local search competitive learning and reverse learning is proposed, which improves the optimization performance of the particle swarm optimization algorithm on complex and high-dimensional optimization problems.

Verifies the outstanding performance of SW-OBLCSO algorithm in convergence speed and segmented search ability.

With large-scale electric vehicles connected to the power grid as the background, the SW-OBLCSO algorithm is adopted, while taking into account economy, environmental protection, safe operation of the power grid and user charging costs, which improves the quality of power grid operation and reduces user charging costs.

This paper is structured as follows. Section 2 gives the optimization goals and constraints. In Section 3, we give optimization algorithms. Set simulation parameters and case, analyze the simulation results in Section 4. We conclude the paper in Section 5.

2. Modeling and mathematical formulating of energy sources planning problem

2.1. Grid power generation system

In the current power generation system of the power grid, in addition to non-renewable energy generating units composed of fossil fuels, wind power and solar power generation are the two main renewable energy power generation. With the popularity of EVs, EVs with vehicle-to-grid (V2G) capabilities can feed electrical energy back to the grid when the state of charge (State of Charge, SOC) is high, V2G technology has brought a large-scale energy storage capacity to the power grid, which will alleviate the increasing power supply pressure of the power grid, and play a key role in solving the problem of "peak shaving and valley filling" of the power grid, regulating the grid load, and improving the efficiency of the power grid. For electric vehicle users, charge the car and store electricity at a low price during the low electricity consumption period, and use a higher electricity price to deliver electricity to the grid during the peak period of electricity consumption. The difference between the low and peak electricity price can be provided to the car owner. Bring certain economic benefits, thereby further reducing the charging cost of electric vehicle owners.

2.1.1. Wind power modeling

Wind power does not have the characteristics of stable output power of thermal power units. Its output power depends on the wind. It has obvious characteristics of randomness, intermittentness and unschedulability. When large-scale wind power is connected, its power fluctuation is often related to the fluctuation of electricity load. On the contrary, this anti-peak shaving feature increases the difficulty of power grid dispatch, affects the real-time balance of power, and then threatens the safe operation of the power grid, and ultimately leads to the occurrence of wind abandonment. Wind curtailment not only causes a great waste of energy, but also seriously affects the economics of wind farm operation. Therefore, in the context of large-scale electric vehicle access, research on wind power forecasting methods to reduce wind farm output power forecast errors will improve the level of wind power absorption, help wind power development, reduce unnecessary wind curtailment from the power grid, and ensure that electric vehicles and power grids Orderly interaction and safe and stable economic operation of the power grid are of great significance.

Short-term wind power prediction is to establish a power prediction model based on historical information such as wind farm environmental factors, output power, wind speed, and wind direction, and use probability statistics to obtain wind power output power for a period of time in the future. In order to improve the description and calculation efficiency of the scene, it is necessary to reduce the scene so that the probability distance between the reserved scene set and the scene set before the reduction is the smallest, and finally the wind power output predicted power value and each wind power output with the smallest error in each time period and closer to the real situation are obtained,the probability value of the wind power scene. The probability value of the wind farm power scene and each wind power scene adopts the prediction results of the literature [27], the scene probability of wind power scene 10 is the largest, and its probability value is 0.086, this article uses the result of scene 10.

Fig. 1 demonstrates a conventional power curve of a wind turbine.

$$P_i = \begin{cases} 0 & 0 \le SW_i \le V_{ci} \\ P_r \times \left(A + B \times SW_i + C \times SW_i^2\right) & V_{ci} \le SW_i \le V_r \\ P_r & V_r \le SW_i \le V_{co} \\ 0 & SW_i \ge V_{co} \end{cases} \quad (1)$$

In this paper, a typical wind power generation model speed of 3.8, 13.5 and 24 meters per second with connection, rated and disconnection respectively, and maximum output of 1.2 MW.

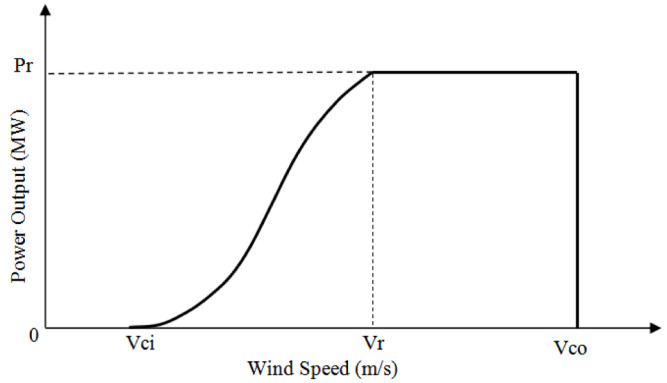

Fig. 1. Conventional wind curve of a wind turbine.

2.1.2. Solar power modeling

As a green and renewable resource, the scale of solar energy is increasing. However, due to the uncertainty of solar energy, the demand response characteristics of participating in the operation of the power grid are also showing large uncertain characteristics, which greatly increases the risk of the operation of the distribution network.

In this paper, electric energy conversion function as follows:

$$P = \eta^{PV} \times S^{PV} \times g \tag{2}$$

Where, g determines the solar radiation, η^{PV}, S^{PV} are solar cells efficiency and total area of solar respectively.

2.1.3. EVs

EVs have the characteristics of zero pollution, low energy consumption, and expanded use of renewable energy, EVs have obvious advantages in energy saving and emission reduction, but the continuous increase in the number of grid-connected and battery capacity has brought a huge operating burden to the power system. The disordered charging and discharging behavior of EVs coincides with the peak value of the grid load curve, which will aggravate the problem of grid overload, the disorderly grid connection of a large number of EVs will bring reliability and safety hazards to the grid, such as increased peak load, increased network loss, overloaded transmission lines, accelerated transformer aging, etc.

2.2. Optimize the target

Fully consider the energy generation structure of renewable energy and non-renewable energy, EV can participate in the optimal dispatch of the grid, reduce the load pressure, and the safety indicators of stable operation of the grid, this paper formulates four indicators for operating costs, pollution emissions, grid operation optimize and user charging cost the target.

2.2.1. Operating costs

The operation cost mainly includes two parts as follows:

$$F_1 = F_{11} + F_{12} \tag{3}$$

$$F_{11} = C_{FC,Diesel(DG)} \tag{4}$$

$$F_{12} = \sum_{t=1}^{T} P_{Gird(t)} \times C_{Grid(t)} \tag{5}$$

In formula (4), $C_{\mathrm{FC,Diesel\ (DG)}}$represent the operating costs of non renewable energy (fuel cells and diesel generators), in formula (5), $P_{Grid\ (t)}$ $C_{Grid\ (t)}$represent the active power and electricity price in time t respectively.

2.2.2. Carbon emission

The pollution function as follows:.

$$F_2 = F_{21} + F_{22} \tag{6}$$

$$F_{21} = Em^{DG} = \sum_{t=1}^{T} \sum_{DG=1}^{N_{DG}} P_{DG(DG,t)} \times E_{CO_2}^{DG,t}, \forall t \in \{1, \ldots, T\}, \forall DG \in \{1, \ldots, N_{DG}\} \tag{7}$$

$$F_{22} = Em^{Grid} = \sum_{t=1}^{T} P_{Grid(t)} \times E_{CO_2}^{Grid,t} \tag{8}$$

$F_{21}$is carbon dioxide pollution of diesel generator(from t=1 to t=T), F_{22}function demonstrates the pollution associated with power generation units in grid,the unit of carbon dioxide emission is kg.

$$E_{CO_2} = aver \times fac \times (1-k)\left(u_j + v_j P_{j,t} + w_j P_{j,t}^2\right) \tag{9}$$

In formulas (8) and (9), *aver* represents the received base ash content of coal, 20 is generally used for calculation, *fac* represents coal ash conversion coefficient, 5.1 is used for calculation, and k represents the pollution removal rate of control measures,take 0.99, $P_{j,t}$ is the active power output by generator set j at time t, u_j,$v_j$and w_j are the coal consumption characteristic coefficients of the generator respectively.

In order to facilitate the solution of this problem, this paper adopts a weighted sum method for operating costs and pollution emissions.

$$\min F_{1,2} = \lambda_1 F_1 + \lambda_2 C F_2 \tag{10}$$

In formula (10), λ_1, λ_2 is the weighting factor, C is the unit cost of carbon emissions, the unit is RMB (yuan) .

2.2.3. Grid operation indicators

The F_{31} is load fluctuation variance, the $F_{32}$is load peak-valley difference, sum of voltage offsets of each node is F_{33}, power grid loss is F_{34}, the expressions are as follows:

$$F_{31} = \sum_{j=1}^{t} \left[P_j + P_L - L_{av}\right]^2 \tag{11}$$

$$F_{32} = \max_{1 \le j \le t} P_j - \min_{1 \le j \le t} P_j \tag{12}$$

$$F_{33} = \sum_{t=1}^{t_N} \sum_{i=1}^{N_{node}} \left(U_i^t - U_i^b\right) \tag{13}$$

$$F_{34} = \sum_{t=t_1}^{t_N} \sum_{l=1}^{l_{\max}} \left(I_{l,t}^2 R_l\right) \Delta t \tag{14}$$

Among them,P_j is the equivalent load of the distribution grid system of the electric vehicle at the time j, $P_L$is the original load when the charging load of the EV is not included in the distribution grid. and L_{av}represents the average daily load of the distribution grid. U_i^trepresents the actual operating voltage of node i period t, and U_i^b represents the rated voltage of node i. R_l is the line resistance of branch l in the distribution grid, $I_{l,t}$is the current of branch l in the distribution grid in the time period, $l_{\max}$ is the total number of branches in the distribution grid.

2.2.4. User charging cost

$$F_4 = \sum_{t=1}^{T} \sum_{V=1}^{N_V} P_{Charge(V,t)} \times C_{Charge(V,t)} - P_{Discharge(V,t)} \times C_{Discharge(V,t)} \tag{15}$$

In formula (15) $P_{Dis\ charge\ (V,t)}$, $P_{Charge\ (V,t)}$, $C_{Dis\ charge\ (V,t)}$, $C_{Charge\ (V,t)}$respectively represents the discharge, charging power, discharge and charging price of the v-th EV in the time t.

2.3. Problem constraint

$$P_{Grid\,(t)} + \sum_{DG=1}^{N_{DG}} P_{DG(DG,t)} + \sum_{wind=1}^{N_{wind}} P_{wind(DG,t)} + \sum_{PV=1}^{N_{PV}} P_{PV(DG,t)} + \sum_{V=1}^{N_V} P_{Dis\,charge(V,t)} = D_t + \sum_{V=1}^{N_V} P_{Charge\,(V,t)} + Loss_t \tag{16}$$

$$\forall t, i : V_{\mathrm{imin}} \le V_{i,t} \le V_{\mathrm{imax}} \tag{17}$$

$$\forall i, j, t \begin{cases} P_{G(i,t)} - P_{l(i,t)} = V_i \sum_{j=1}^{n} V_j \left(G_{ij}\cos\theta_{ij} + B_{ij}\sin\theta_{ij}\right) \\ Q_{G(i,t)} - Q_{l(i,t)} = -V_i \sum_{j=1}^{n} V_j \left(G_{ij}\sin\theta_{ij} - B_{ij}\cos\theta_{ij}\right) \end{cases} \tag{18}$$

Formula (16) is the power balance constraint, formula (17) is the voltage amplitude constraint, formula (18) is the power flow constraint.

Among them, D_t is the basic load of the system in time period t, $Loss_t$ is the network loss of the system in time period t. i and j are node numbers, $V_{\mathrm{imax}}, V_{\mathrm{imin}}$are the upper and lower limits of the voltage operation of node i, $V_{i,t}$is the real-time voltage of node i at time t. $P_{l(i,t)}$, $Q_{l(i,t)}$are the active and reactive power injected into node i at time t; $P_{G(i,t)}, Q_{G(i,t)}$ are the active and reactive power of generator at time t node i.n represents the number of nodes in the system, $\theta_{ij}$is the phase angle difference of branch ij, $G_{ij}$and$B_{ij}$are the real and imaginary parts of the i-th row and j-th column of the node admittance matrix.

3. SW-OBLCSO algorithm

3.1. PSO algorithm

PSO algorithm is a common swarm intelligent optimization algorithm. Its basic idea is to simulate the foraging process of birds. Each bird is equivalent to a possible solution of the optimization problem, the flight space of birds is equivalent to the search area of the optimization problem, and the food represents the optimal solution of the problem. In the search process, the initial population is composed of a group of randomly generated particles, then each particle in the initial population updates its speed and position according to the formula shown in formula (19) and formula (20), finally reaches the optimal position after a certain number of iterations, the normal PSO can be defined by Shi and Eberhart [2]:

$$v_{id}^{k+1} = \omega * v_{id}^{k} + c_1 * r_1\left(p_{id}^{k} - x_{id}^{k}\right) + c_2 * r_2\left(p_{gd}^{k} - x_{id}^{k}\right) \tag{19}$$

$$x_{id}^{k+1} = x_{id}^{k} + v_{id}^{k+1} \tag{20}$$

Where, $\omega$is the inertia weight coefficient, $c_1, c_2$is the learning factor; r_1, r_2 is the random number between 0 and 1;x_{id}^{k} is the current position of the particle in the i-th dimension in the k-th iteration; $p_{id}^{k}$is the individual extremum; $p_{gd}^{k}$is the optimal solution found by the whole particle swarm.

The selection of PSO algorithm parameters is very important, at present, there are two main categories: fixed and time-varying, the former model is simple, running fast, but the accuracy is not high, it is easy to fall into local extremes, and the adaptability is poor; the latter has complex models and slow running speed, but the accuracy is high and it has a certain degree of adaptability. In order to have the advantages of both and avoid their disadvantages, it is necessary to improve the PSO algorithm.

3.2. Improvement of PSO algorithm

In order to further improve the solution effect of the PSO algorithm, the algorithm's global search ability and local search ability can reach a better balance. Based on the particle swarm algorithm, this paper combines the reverse learning mechanism and local search strategy, adopts the reverse learning competitive particle swarm optimization algorithm based on local search (SW-OBLCSO), the improved competition mechanism combined with the reverse learning mechanism improves the convergence speed of the algorithm. In the later stage of the search, combined with the individual-based local heuristic search operator to help the algorithm jump out of the local optimal solution.

3.2.1. Solis & wets local search (SW) algorithm

The local search algorithm is a meta-heuristic algorithm commonly used to solve optimization problems, the local search starts from an initial solution, and then explores its neighborhood, if a better solution is found, move to the solution and continue the search, otherwise keep the current solution. The local search algorithm is a powerful local search algorithm, which belongs to the random hill climbing algorithm with adaptive step size. Its performance has been verified in many large-scale optimization algorithms.

3.2.2. Opposition-based learning

Opposition-Based Learning (OBL) is a mechanism proposed by Tizhoosh that can effectively broaden the search space and cover the feasible solution area, it has been effectively used in differential evolution algorithms, the reverse learning mechanism can calculate candidate solutions and their corresponding reverse solutions in a single iteration. The advantage of introducing the reverse learning mechanism is that it can search for the current point and the reverse point at the same time. If the fitness value of the reverse point is excellent based on the fitness value of the current point, the particles can directly jump to the reverse point or its neighborhood to continue searching, which can quickly expand the solution space and increase the possibility of finding the global optimal solution.

3.2.3. Competitive learning mechanism

In the PSO algorithm, as the evolution process progresses, the individual historical best position of the particle may have the same value as the global best particle, resulting in a decrease in the diversity of the population. In order to weaken or eliminate the influence of the global best particle and the best particle in individual history, the competitive swarm optimizer (CSO) can be used to solve the problem, in which the particles are updated through continuous random pair-wise competition. After the pair-wise competition, the winner particle directly passed to the next iteration, the loser particles learn from the winner particles, and finally the algorithm obtains stronger optimization performance.

In the competitive particle swarm algorithm, the particles do not have the memory function, and the algorithm is not easy to fall into the local optimum during the optimization process. The reverse learning is also an effective mechanism to broaden the search space. In order to make full use of the advantages of the two mechanisms, further improve optimization performance of the algorithm, based on the competition mechanism, fully combines the characteristics of the reverse learning mechanism and the local search algorithm to make the algorithm performance better.

3.3. Reverse learning competitive particle swarm optimization (SW-OBLCSO) algorithm based on local search

In the iterative process of the algorithm, the population is randomly divided into four groups each time, each group selects a particle in turn for fitness evaluation, and then sorts it according to the fitness value. The first-ranked particle directly enters the next generation and is called the winner; the second-ranked particle learns in reverse; the third-ranked particle competes and learns from the winner particle; the last-ranked particle obtains the position of the winner particle and adds a bias set the amount to increase the convergence speed and maintain the

diversity of the population. After all the particles in the four groups participate in the competition, find the minimum fitness value in the group at this time. If the minimum fitness value does not change for multiple consecutive generations, then SW search is performed on the particle with the minimum fitness in the subsequent iterations, the SW deviation vector d becomes smaller as the number of iterations increases. The second, third, and fourth (Loser) fitness values of the particles in the SW-OBLCSO algorithm update their position and velocity through following formulas:

$$V_{td}^{k}(t+1) = R_{1d}^{k}(t)\cdot V_{td}^{k}(t) + R_{2d}^{k}(t)\left(X_{wd}^{k}(t) - X_{td}^{k}(t)\right) + \varepsilon\cdot R_{3d}^{k}(t)\cdot\left(\widetilde{X}_{d}^{k}(t) - X_{td}^{k}(t)\right) \tag{21}$$

$$X_{td}^{k}(t+1) = X_{td}^{k}(t) + V_{td}^{k}(t+1) \tag{22}$$

$$X_{sd}^{k}(t+1) = hb_d + lb_d - X_{sd}^{k}(t) + R_{4d}^{k}(t)\cdot X_{sd}^{k}(t) \tag{23}$$

$$X_{ld}^{k}(t+1) = X_{wd}^{k}(t) \pm \tanh'i\cdot f_d(t) \tag{24}$$

Among them, $X_{sd}^{k}(t), X_{td}^{k}(t)$and $X_{ld}^{k}(t)$represent the second, third, and d-th dimension of the position of the loser in the k-th round of the t-th iteration, respectively. $V_{td}^{k}(t)$is the speed of the dth dimension of the third place in the k-th round of the t-th iteration. $R_{1d}^{k}(t), R_{2d}^{k}(t), R_{3d}^{k}(t)$ and $R_{4d}^{k}(t)$are four random numbers in [0, 1], ε is a manually set parameter, $\widetilde{X}_{d}^{k}(t)$ is the average position of all particles, $hb_d$and $lb_d$are the upper and lower bounds of the d-th dimension of the search space,$f_d(t)$is the d-th dimension in the t-th iteration of the Gaussian sampling deviation vector with the same dimension as the problem, i is a constant. On the basis of the winner, two new solutions$x + \tanh'i\cdot f_d(t)$and$x - \tanh'i\cdot f_d(t)$ are generated, the fitness values of the two new solutions are calculated, a better solution is selected and assigned to the loser, the algorithm flow of SW-OBLCSO is as follows:

Step 1: Initialize the population P, the position and velocity of the particles
Step 2: WHILE FEs<max_FEs
Step 3: Randomly disrupt the population and divide it into four groups
Step 4:for k=1:N/4 do
Take out one particle from each group and mark it as (r1, r2, r3, r4), (w, s, t, l) = compete(r1, r2, r3, r4).Update the position and velocity of the particles according to formulas (21–24). Update the fitness value of the second, third, and fourth place
Step 5:end for
Step 6: Find the optimal fitness particle of the population and record [min_index, min_fit]
Step 7: If the value of min_fit does not change continuously for N times, perform a SW partial search on P(min_index)
Step 8: END WHILE

3.4. Comparison and analysis of algorithm results

The algorithm combines reverse learning and local search on the basis of an improved competition mechanism. Compared with the CSO algorithm, it is equally simple but more effective. In the algorithm iteration process, the population is randomly divided into four groups each time, and each group selects one particle in turn for adaptation The first-ranked particle directly enters the next generation and is called the winner; the second-ranked particle performs reverse learning; the third-ranked particle competes and learns from the winner particle, and the last ranked particle The particle obtains the position of the winner particle and adds a bias to increase the convergence speed and maintain the diversity of the population. After all the particles in the four groups participate in the competition, find the minimum fitness value in the group at this time, if there are more consecutive If the minimum fitness value of the generation does not change, the SW search is performed on the particles with the minimum fitness in the subsequent iterations, where the SW deviation vector d decreases as the number of iterations increases.

In order to test the optimization ability and convergence efficiency of the SW-OBLCSO algorithm proposed in this paper, four detection functions commonly used in algorithms in the field of computational intelligence are selected as the algorithm test functions.

3.4.1. Test function

The function$f_1$is a typical ill-conditioned unimodal function, the algorithm has a small chance of finding the global optimum, $f_2$is the step function, when the function approaches infinity in the domain of definition, different step phenomena will appear at a given interval, there will be a large number of local extrema between each step; the function $f_3$is an inseparable rotatable function, the surface of the function has a large number of crests and troughs, the optimization algorithm is easy to fall into the local optimum on the path to the global optimum, f_4 is a function with a lot of noise. The expressions of these four test functions are as follows:

$$f_1(x) = \sum_{i=1}^{D-1}\left[100\left(x_i^2 - x_{i+1}\right)^2 + \left(x_i - 1\right)^2\right] \tag{25}$$

$$f_2(x) = \sum_{i=1}^{D-1}\left[\left(x_i + 0.5\right)^2\right] \tag{26}$$

$$f_3(x) = \sum_{i=1}^{D} x_i^2 \Big/ 4000 - \prod_{i=1}^{D}\cos\left(x_i \Big/ \sqrt{i}\right) + 1 \tag{27}$$

$$f_4(x) = \sum_{i=1}^{D} x_i^4 * i + rand[0, 1] \tag{28}$$

3.4.2. Algorithm comparison

Choose PSO algorithm, QPSO algorithm [30] and RDPSO algorithm, SLPSO algorithm [31,32], OBLCPSO algorithm, CSO algorithm, these latest improved algorithms as the comparison algorithm. In order to test the optimization performance of SW-OBLCSO algorithm on low-dimensional problems and the expansion performance of high-dimensional problems, the dimensions of the four basic test functions are set to D=100, 500, 1000. Due to the change of the problem dimension, the population size of each algorithm is set to N=M+D/10 and M=100, in order to reduce the randomness of the experiment, each algorithm runs randomly and independently on each test function 25 times, each experiment uses the maximum number of evaluations (max FEs) as the termination condition, max FEs=200,000. The algorithm parameter settings used are shown in Table 1.

Fig. 2 shows the convergence curve of each algorithm optimized for each test function in the case of 100 dimensions. The abscissa is the number of evaluations. For test functions$f_1$and$f_4$with large changes in fitness values, the ordinate is the natural logarithm of the average fitness

Table 1
Parameter settings of each comparison algorithm.

Algorithms	Parameter settings
SW-OBLCSO	ε=0.7, i=20, N=50, $maxS$=5, $maxF$ =3, adS=2, adF =0.5, dev=$\tanh'(t/120)$
PSO	ω=0.95–0.38, $c_1 = c_2 = 2.0$
CSO	ε=0.7
OBL-CPSO	ε=0.7–0.2
SLPSO	α=0.5, β=0.01
RDPSO	ω=0.9–0.3, $c_1 = c_2 = 1.5$
QPSO	α=0.5–1

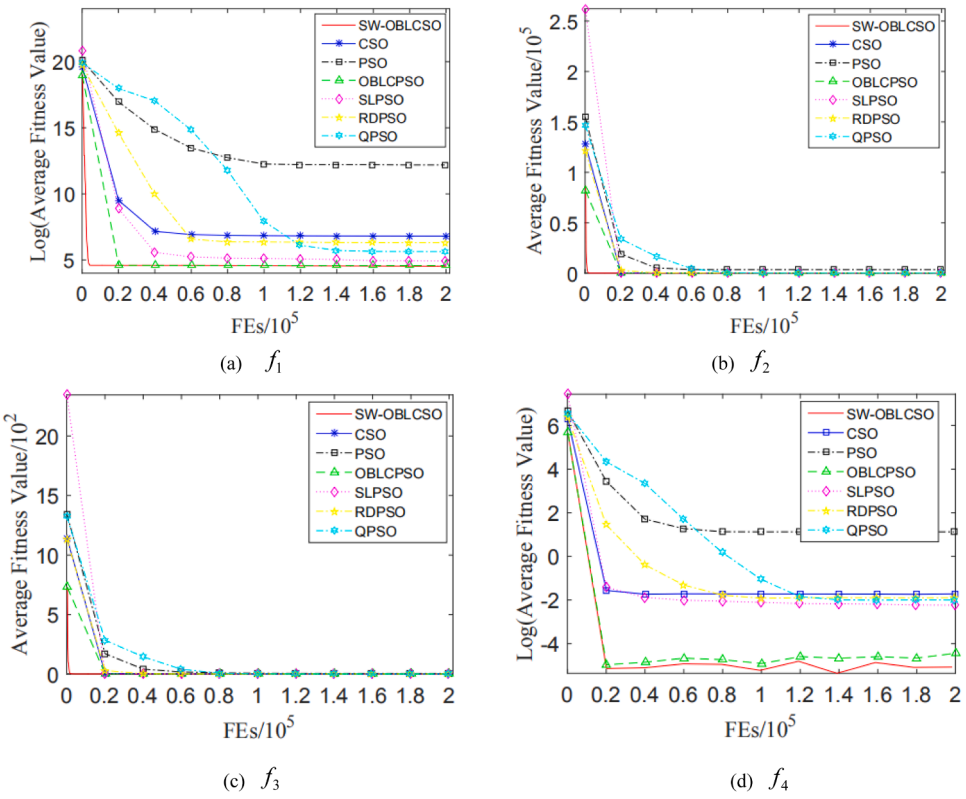

Fig. 2. The convergence curve of each algorithm optimization in the test function (100 dimensions).

value, the ordinates of the test functions $f_2$and f_3 are the average fitness values.

It can be seen from the convergence curve that with the intervention of the local search strategy, the SW-OBLCSO algorithm jumps out of the local optimum, and the convergence speed has been significantly improved. It can be seen that the introduction of the competition mechanism and the reverse learning mechanism makes the SW-OBLCSO algorithm have extremely high search efficiency, due to the combination of the local search algorithm, the algorithm has high optimization accuracy at the same time, and can be evaluated in a few times, find the best overall advantage.

The experimental results of SW-OBLCSO algorithm and comparison algorithm on 4 test functions are given in Table 2. The experimental results of each test function are composed of three rows of data, which represent the optimization results in 100, 500, and 1000 dimensions respectively. There are two columns for each algorithm. The first column represents the average value of the objective function obtained by the algorithm running 25 times in this dimension on the test function, and the second column represents the standard deviation of the 25 objective function values.

From the experimental data in Table 2, it can be seen that the optimization performance of the SW-OBLCSO algorithm proposed in this paper on the four test functions is generally better than the other six algorithms, and the standard deviation of the optimization results is small. Compared with the OBLCPSO algorithm, the SW-OBLCSO algorithm is found to have better performance in the test function f_4 under 100 dimensions, in the remaining 3 test functions, the optimization performance of the two algorithms is equivalent, in the 500 and 1000 dimensions, the performance of the SW-OBLCSO algorithm in the test function f_1 is superior, the performance in the test function f_4 is not as good as the OBLCPSO algorithm, and the optimization performance of the two on the test functions f_2 and f_3 is equivalent. Compared with the other five algorithms, the SW-OBLCSO algorithm has certain advantages in the optimization performance of the four test functions in each dimension. In addition, it can be seen that as the dimensionality increases, the SW-OBLCSO algorithm can still maintain good optimization performance and has good high-dimensional scalability. It can be seen from the convergence curve that the two algorithms using reverse learning have the fastest convergence speed on most test functions, especially on the test functions f_2 and f_3, which can find the overall situation in a few evaluation times, the best advantage, it also proves that the combination of reverse learning mechanism and PSO method is effective.

In summary, Thanks to the special competition mechanism and reverse learning mechanism, the SW-OBLCSO algorithm has a very high search efficiency; combined with the SW local search algorithm, the algorithm also has a high optimization accuracy.

4. Case and simulation result

4.1. Parameter setting

This paper analyzes the charging situation of EVs in IEEE-33 node distribution grid, 22.6 kV distribution bus which is shown in Fig. 3, the number of EVs participating in distribution grid is 3000.

The daily load curve of the distribution network studied in this paper is shown in Fig. 4.

For non-renewable energy power generation, the expression of its operating cost is as follow:

$$C_{(j,t)} = a_j + b_j P_{(j,t)} + c_j P^2_{(j,t)} \tag{28}$$

$P_{(j,t)}$ is the active power of generator set j at time t, a_j,$b_j$and$c_j$are the cost coefficients of generator j, respectively.

Pollution emissions are related to power generation. In order to facilitate processing, the pollution emissions of fuel cells and diesel units in the distribution system are shown in Table 3.

In Table 3, P_{max} represent the maximum generating power of the unit.

Table 2
Experimental results of each algorithm on the test function.

Test function	Test dimension	SW-OBLCSO (this paper)		PSO		CSO		OBL-CPSO	SLPSO		RDPSO		QPSO	
f_1	100	9.2E+01	1.2E+00	2.0E+05	4.6E+05	9.1E+02	2.5E+02	9.7E+01	5.1E-01	1.4E+02	6.1E+01	5.4E+02	1.3E+02	2.8E+02	8.3E+01
	500	5.1E+02	1.3E+01	2.9E+08	3.7E+07	1.2E+06	2.2E+05	5.1E+02	2.2E-01	1.3E+07	2.5E+06	4.5E+07	6.8E+06	2.6E+07	4.4E+06
	1000	9.9E+02	2.7E+00	1.1E+09	1.1E+08	5.1E+06	4.5E+05	9.9E+02	2.1E-01	7.1E+08	2.7E+07	3.1E+08	2.5E+07	2.6E+08	2.6E+07
f_2	100	0	0	3.5E+03	1.9E+03	2.2E+01	1.1E+01	0	0	5.2E-01	9.2E-01	1.6E-01	2.1E+01	1.2E+01	7.8E+01
	500	0	0	2.1E+05	1.4E+04	9.5E+03	1.1E+03	0	0	3.4E+03	4.1E+02	5.1E-04	6.8E+03	2.9E+04	4.6E+03
	1000	0	0	6.4E+05	2.5E+04	3.3E+04	1.9E+04	0	0	2.7E+05	9.1E+03	2.3E+05	1.5E+04	1.8E+05	1.5E+04
f_3	100	0	0	5.1E+00	3.1E+00	4.5E-01	3.3E-01	0	0	2.1E-03	5.5E-03	1.8E-01	2.2E-01	2.1E-02	3.4E-02
	500	0	0	1.7E+03	1.6E+02	7.9E+01	1.2E+01	0	0	3.1E+01	4.9E+00	4.3E+02	6.3E+01	2.2E+02	2.4E+01
	1000	0	0	5.5E+03	2.4E+02	2.8E+02	1.7E+01	0	0	2.4E+03	9.4E+01	2.1E+03	1.6E+01	1.6E+03	1.3E+02
f_4	100	4.6E-03	5.1E-03	3.1E+00	1.7E+00	1.8E-01	4.9E-02	1.2E-02	1.3E-02	1.1E-01	1.7E-01	1.5E-01	3.7E-02	1.4E-01	3.1E-02
	500	6.7E-03	6.4E-03	1.9E+03	2.9E+02	1.3E+01	2.3E+00	5.8E-03	4.6E-03	5.9E+01	1.1E+01	2.7E+02	6.5E+01	1.8E+02	3.9E+01
	1000	5.3E-03	5.6E-03	1.7E+04	1.7E+03	7.3E+01	9.3E+01	3.6E-03	3.7E-03	8.3E+03	5.1E+02	4.0E+03	4.6E+02	3.4E+03	3.4E+02

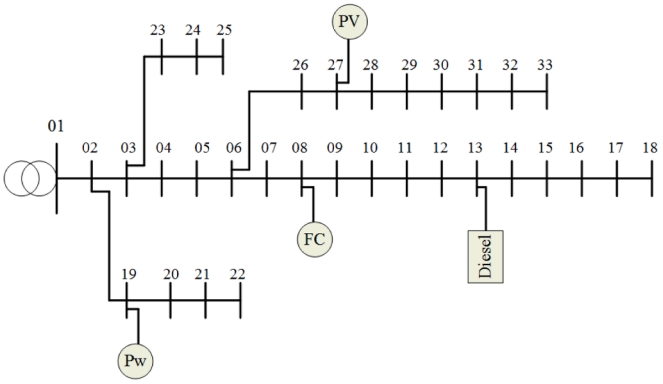

Fig. 3. Standard 33-bus radial distribution Grid.

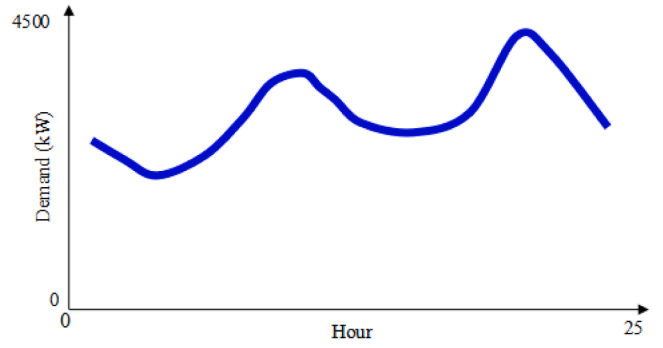

Fig. 4. Total electric load curve in studied grid.

Table 3
Non-renewable sources information.

Plant	Price coefficients			Constrains	Pollutions
	a	b	c	$P_{max(kW)}$	kg
Diesel Gen.	10	0.0133	0.002	1000	0.89
Fuel Cell	45	0.375	0	1000	0.477

The battery specifications of all EVs are the same, charging and discharging once a day, the charging time is 6 hours, the discharging time is 5 hours, and the charging and discharging power of EVs is 3.6 kW. In this paper, the charging and discharging of EVs adopts the dynamic electricity price mode, the electricity price of each period is shown in Table 4.

4.2. Simulation analysis

4.2.1. Minimize operating costs and pollution emissions

Using SW-OBLCSO algorithm, under the condition of minimum operation cost and pollution, the best obtained answer from this method and the results of distributed generation sources planning is shown in Fig. 5.

The voltage profile is depicted in Fig. 6.

Fig. 7 shows the voltage profile improvement in case of connection of EVs and distributed sources to the grid.

Table 5 lists the operation cost and pollution before and after optimization, which are obviously greatly reduced through optimization

The results show that when EVs are connected to the grid, they can be charged at times when electricity prices are low, while reducing pollution.

Table 4
Charge and discharge price.

Hour	1	2	3	4	5	6	7	8	9	10	11	12
Price (Yuan)	0.55	0.47	0.47	0.47	0.47	0.55	0.55	0.62	0.71	0.79	0.79	0.79
Discharge (Yuan)	0.65	0.47	0.47	0.47	0.47	0.55	0.75	0.80	0.95	1	1	1
Hour	13	14	15	16	17	18	19	20	21	22	23	24
Price (Yuan)	0.71	0.71	0.79	0.79	0.93	0.71	1.17	1.25	1.25	1.17	1.01	0.78
Discharge (Yuan)	0.95	0.95	1	1	1.2	0.95	1.35	1.5	1.5	1.35	1.1	1

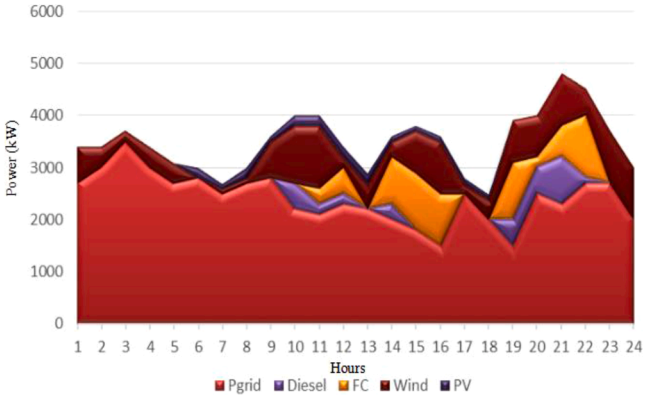

Fig. 5. Planned power of distributed energy sources.

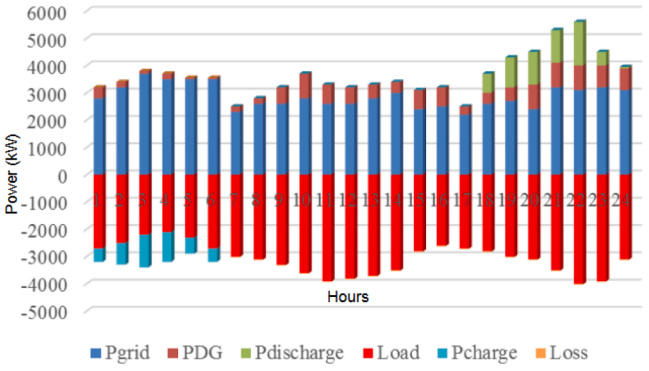

Fig. 6. Power balance curve.

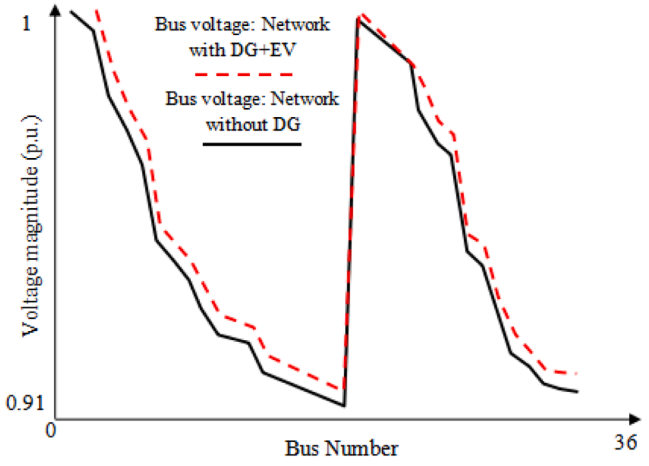

Fig. 7. Voltage profile in distribution grid.

Table 5
Optimization Results.

Grids	Operation costs (Yuan)	Emission costs (kg)
Traditional Net.	58,353.2	33,346
Optimization	24,335.8	16,678

4.2.2. Power grid operation index simulation

In the simulation of grid operation indicators, this paper compares the two states before and after the SW-OBLCSO algorithm is used for charging EVs connected to the grid.

For the convenience of observation, the number of EVs that can be charged at each grid access time is converted into the percentage of the number of EVs to the total number of vehicles entering the grid. The optimization results obtained by the simulation are shown in Table 6.

The Fig. 8 below shows the fitting curve of disordered charging and ordered charging load.

Comparing the Fig. 8, it can be seen that the load fluctuates greatly between 13:00–16:00 during disordered charging, and the ordered charging plays a good role in suppressing the fluctuation of the load; the orderly charging process is cut off two load peaks appearing at 14:00 and 21:00; the orderly charging method shifts the EVs charging load from the peak load period (17:00–21:00) to the load valley period (23:00–6:00).

It can be seen from Table 7 that after the orderly charging, the load valley value is increased by 877 kW compared with the disordered charging, and the peak value is decreased by 929 kW, which reduces the peak-to-valley difference from 12,692 kW to 10,886 kW in the disordered charging, which is reduced by 1806 kW, it is effectively realized, the peak-filling of the daily load and the increase in the utilization rate of the equipment are conducive to the economic operation of the grid.

Since the charging load peak period is at 19:00, the voltage of each node of IEEE-33 during the peak charging period is as shown in the Fig. 9 .

It can be seen from Fig. 9 that when the load reaches the peak value for disorderly charging, the voltage per unit value of node 15–18 is lower than 0.9, and the security of the power grid is affected. After adopting the optimized solution, it can be kept within the standard working range of the voltage, ensure the reliable operation of the power grid.

Table 8 shows the values of three objective functions of total loss, charge cost and load fluctuation of distribution grid under different charging modes.

In this simulation, a single target is first tested under constraint conditions, the comprehensive optimization of multiple objectives still uses the weighted sum method.

It can be seen from Table 8 that the index values under random charging mode are poor, which will have a greater impact on the distribution grid.

Although single-objective optimization can make one indicator obtain the optimal value, it usually cannot guarantee that other indicators are at a better level. First, ensure the power quality, ensure that the voltage of each node does not exceed the limit, and reduce the line loss of the power grid; secondly, accelerate the popularization of EVs and reduce the charging cost of users; finally, minimize the fluctuation of the equivalent load of the power grid and improve the economic

Table 6
The total number of EVs that can be charged at the moment of access into the grid.

Permeability/%	The number of EVs /%									
	0	1	2	8	10	13	18	19	22	23
50	25	23	36	0	0	0	0	0	3	13
100	14	14	28	4	1	12	2	6	8	11
50	14	19	13	9	0	45	0	0	0	0
100	11	12	9	24	0	42	0	0	0	2

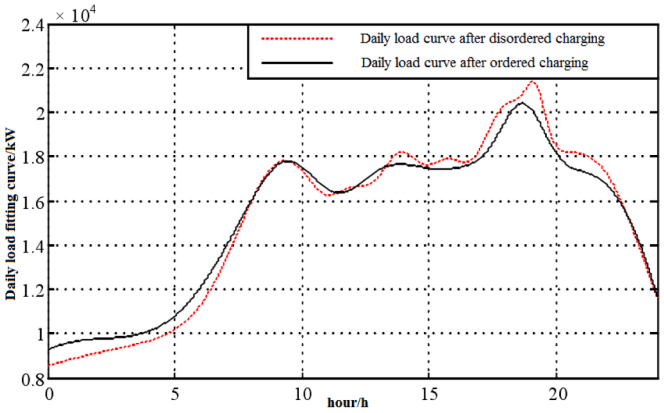

Fig. 8. Daily load curve after ordered/disordered charging.

Table 7
Comparison of daily load curve of disordered charging and ordered charging of EVs.

Daily load curve	Valley (kW)	Peak (kW)	Peak-to-Valley Difference (kW)	Load Rate (%)
Daily load after disordered charging	8697	21,389	12,692	67.81
Daily load after orderly charging	9574	20,460	10,886	75.02
Daily load change value	877	-929	-1806	7.21

operation of the power grid. It can be seen from Table 8 that the comprehensive solution obtained by considering the equivalent load fluctuation and total loss of the distribution network and the charging cost of EV users is more practical, the data in Table 8 verifies this point well. The optimal balance can be achieved under the bilateral constraints of the grid side and the user side, and the bilateral benefits can be maximized.

5. Conclusion

In this paper, from the perspective of grid operation and EV charging users, taking IEEE-33 node distribution grid system as an example, a multi-objective optimal regulation strategy is proposed to achieve the following objectives: the lowest grid operation cost, the lowest pollution, the minimum peak valley difference, the minimum sum of voltage offsets of each node, the minimum distribution grid loss and the minimum charging cost. The improved multi-objective particle swarm optimization algorithm is used to solve the problem, on the basis of the PSO algorithm, this paper proposes the SW-OBLCSO algorithm, the algorithm

Table 8
Target function values under different charging modes.

Permeability	System type	Power grid loss (10^4kWh)	Charge Cost (Yuan)	Power grid load fluctuation (kW^2)
	Random charging	2.943	3120	157,641
50%	Optimal solution of total loss of power grid	2.576	1200	96,815
	Optimal solution of charging cost	2.588	740	135,838
	Optimal solution of load fluctuation in power grid	2.588	1869	69,615
100%	Optimal solution of total loss of power grid	2.991	1848	57,672
	Optimal solution of charging cost	3.023	1223	95,399
	Optimal solution of load fluctuation in power grid	3.029	2422	43,025
100%	Multiobjective optimization	3.027	1265	57,842

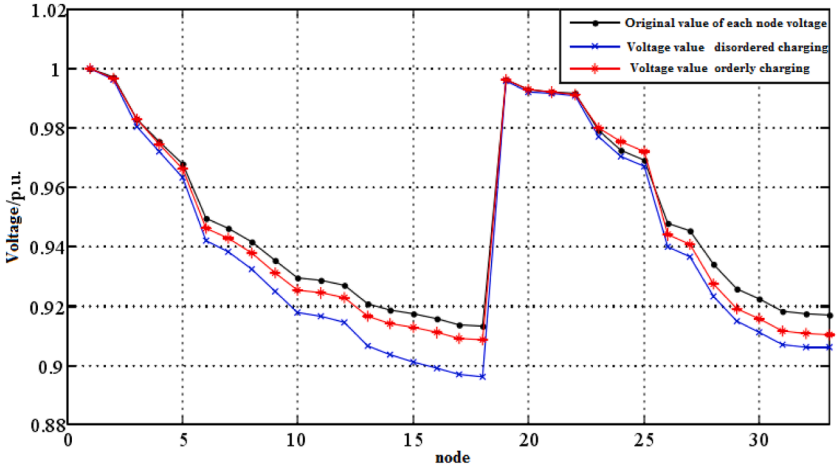

Fig. 9. Ordered/disordered charging node voltage.

uses a combination of competitive learning, reverse learning and local search, which helps the algorithm have good exploration and development capabilities. Through experiments on multiple test functions, results show that the SW-OBLCSO algorithm proposed in this paper is better than the other 6 PSO algorithm variants. The multi-objective orderly charging method described in this paper provides a new way to solve the charging management of EVs in residential areas and commercial buildings and the operation problems after connecting to the power grid, the method can also be extended to the power of regional power grid in the charge and discharge control management of motor vehicles, a new idea is provided for carrying out orderly charge and discharge effectively in the future.

Author statement

I have completed calculation example design, simulation, manuscript writing, etc.;

Ming Zhengfeng completed the manuscript structure planning and algorithm improvement work;

If the manuscript is accepted, we agree to publish it.

Declaration of Competing Interest

We declare that the manuscript has no conflicts of interest.

References

[1] Yin WanJun, et al., Application of new multi-objective optimization algorithm for EV scheduling in smart grid through the uncertainties, J. Ambient Intell. Human. Comput. 04 (2019).

[2] K Qian, C Zhou, M Allan, et al., Modeling of load demand due to EV battery charging in distribution systems, IEEE Trans. Power Syst. 26 (2) (2011) 802–810.

[3] P Zhang, K Qian, C Zhou, et al., A methodology for optimization of power systems demand due to electric vehicle charging load, IEEE Trans. Power Syst. 27 (3) (2012) 1628–1636.

[4] F Marra, G Y Yang, C Traeholt, et al., EV charging facilities and their application in LV feeders with photovoltaics, IEEE Trans. Smart Grid 4 (3) (2013) 1533–1540.

[5] Ali Ashtari, Eric Bibeau, Soheil Shahidinejad, et al., PEV charging profile prediction and analysis based on vehicle usage data, IEEE Trans. Smart Grid 3 (1) (2012) 341–349.

[6] Mustafa A Mustafa, Ning Zhang, Georgios Kalogridis, et al., Smart Electric vehicle charging; security analysis, in: IEEE PES Innovative Smart Grid Technologies (ISGT), Washington DC,USA, 2013.

[7] David Steen, Le Anh Tuan, Ola Carlson, et al., Assessment of electric vehicle charging scenarios based on demographical data, IEEE Trans. Smart Grid 3 (3) (2012) 1457–1468.

[8] G. Li, X.P. Zhang, Modeling of plug-in hybrid electric vehicle charging demand in probabilistic power plow calculations, IEEE Trans. Smart Grid 3 (1) (2012) 492–499.

[9] Jen-Hao Teng, Shang-Wen Luan, Dong-Jing Lee, et al., Optimal charging/discharging scheduling of battery storage systems for distribution systems interconnected with sizeable PV generation systems, IEEE Trans. Power Syst. 28 (2) (2013) 1425–1433.

[10] J.C. Gomez, M.M. Morcos, Impact of EV battery chargers on the power qualityof distribution systems, IEEE Trans. Power Delivery 18 (3) (2003) 975–981.

[11] W Kempton, T.J. Vehicle-to-grid power implementation: from stabilizing the grid to supporting large-scale renewable energy, J. Power Sources 144 (1) (2005) 280–294.

[12] Y Ota, H Taniguchi, T Nakajima, et al., Autonomous distributed V2G (vehicle-to-grid) considering charging request and battery condition, in: IEEE PES Innovative Smart Grid Technologies Conference (ISGT), 2010, pp. 1–6.

[13] N. Rotering, M. Ilic, Optimal charge control of plug-in hybrid EVs in deregulated electricity markets, IEEE Trans. Power Syst. 26 (3) (2011) 1021–1029.

[14] B.A Robbins, C.N Hadjicostis, A.D.A. Dominguez-Garcia, Two-stage distributed architecture for voltage control in power distribution systems, IEEE Trans. Power Syst. 28 (2) (2013) 1470–1482.

[15] Koten Hasan, J. Sigma, Hybrid and EVs for istanbul cycle and drive train design, Eng. Nat. Sci. 9 (4) (2018) 461–470.

[16] M Muratori, G. Rizzoni, Residential demand response: dynamic energy management and time-varying electricity pricing, IEEE Trans. Power Syst. 31 (2) (2016) 1108–1117.

[17] Z Yang, et al., Joint scheduling of large-scale appliances and batteries via distributed mixed optimization, IEEE Trans. Power Syst. 30 (4) (2015) 2031–2040.

[18] M D Galus, et al., Provision of load frequency control by PHEVs, controllable loads, and a con-generation unit, IEEE Trans. Indust. Electron. 58 (10) (2011) 4568–4582.

[19] D Wang, et al., Integrated energy exchange scheduling for multimicro grid system with EVs, IEEE Trans. Smart Grid 7 (4) (2016) 1762–1774.

[20] N Ghiasnezhad Omran, et al., Location-based forecasting of vehicular charging load on the distribution system, IEEE Trans. Smart Grid 5 (2) (2014) 632–641.

[21] Hasan Mehrjerdi, Dynamic and multi-stage capacity expansion planning in microgrid integrated with electric vehicle charging station, J. Energy Storage 29 (2020), 101351.

[22] Hasan Mehrjerdi, Reza Hemmati, Stochastic model for electric vehicle charging station integrated with wind energy, Sustain. Energy Technol. Assess. 37 (2020), 100577.

[23] Hasan Mehrjerdi, Electric vehicle charging station with multilevel charging infrastructure and hybrid solar-battery-diesel generation incorporating comfort of drivers, J. Energy Storage 26 (2019), 100924.

[24] Zhao Xin-gang, Zhang Ze-qi, Xie Yi-min, Meng Jin, Economic-environmental dispatch of microgrid based on improved quantum particle swarm optimization, Energy (2020) 195.

[25] Ran Cheng, Yaochu Jin, A social learning particle swarm optimization algorithm for scalable optimization, Inf. Sci. 291 (2015) 43–60.

[26] Zhang Yufei, Zhao Jianping, Wang Limin, Wu Honggang, Zhou Ruihong, Yu Jinglin, An improved OIF Elman neural network based on CSO algorithm and its applications, Comput. Commun. (2021) 171.

[27] Meiqin Mao, Yong Ding, Liuchen Chang, Nikos D Hatziargyriou, Qiang Chen, Tinghuan Tao, Yunwei Li, Multi-objective power management for EV fleet with MMC-based integration into smart grid, IEEE Trans. Smart Grid (2017).

[28] Christos D. Korkas, Simone Baldi, Shuai Yuan, Elias B. Kosmatopoulos, An adaptive learning-based approach for nearly optimal dynamic charging of electric vehicle fleets, IEEE Trans. Intell. Transp. Syst. 99 (2017) 1–10.

[29] Caroline Le Floch, Emre Can Kara, Scott Moura, PDE Modeling and Control of Electric Vehicle Fleets for Ancillary Services:A Discrete Charging Case, IEEE Trans. Smart Grid 9 (2) (2018) 573–581.

[30] W Fang, J Sun, Y Ding, et al., A review of quantum-behaved particle swarm optimization, IETE Tech. Rev. 27 (4) (2010) 336–348.

[31] R Cheng, Y. Jin, A social learning particle swarm optimization algorithm for scalable optimization, Inf. Sci. 291 (2015) 43–60.

[32] QIAN Xiao-yu, FANG Wei, Opposition-based learning competitive particle swarm optimizer with local search, Control Decis. (2019).